Interconversion of 42- and 44-Electron Platinum *triangulo*-Clusters using Chelating Tertiary Phosphine Ligands and the Structural Characterisation† of [1,3-Bis(diphenylphosphino)propane]-tris(μ-sulphur dioxide)-bis(tricyclohexylphosphine)triplatinum–Benzene (1/2), $[Pt_3(\mu\text{-}SO_2)_3\{P(C_6H_{11})_3\}_2(dppp)]\cdot 2C_6H_6$

Malcolm F. Hallam, Nigel D. Howells, D. Michael P. Mingos,* and Robert W. M. Wardle
Inorganic Chemistry Laboratory, University of Oxford, South Parks Road, Oxford OX1 3QR

The 42-electron *triangulo*-clusters $[Pt_3(\mu\text{-}CO)_3\{P(C_6H_{11})_3\}_3]$ and $[Pt_3(\mu\text{-}SO_2)_3\{P(C_6H_{11})_3\}_3]$ react with chelating phosphines to give 44-electron clusters of the type $[Pt_3(\mu\text{-}X)_3\{P(C_6H_{11})_3\}_2\{Ph_2P(CH_2)_nPPh_2\}]$ (X = CO or SO_2, n = 2 or 3). The molecular structure of the compound $[Pt_3(\mu\text{-}SO_2)_3\{P(C_6H_{11})_3\}_2\{Ph_2P(CH_2)_3PPh_2\}]$ has been determined by single-crystal *X*-ray techniques using diffractometer data. The compound crystallises in the monoclinic space group $P2_1/n$ with four formula units in a cell of dimensions a = 11.244(6), b = 41.746(3), c = 16.324(2) Å, and β = 98.51 (3)°. Least-squares refinement of the structure has led to a final R value of 0.060 using 4 506 unique absorption-corrected reflections with $I \geqslant 3\sigma(I)$. The structure shows an approximately isosceles triangle of platinum atoms; Pt–Pt 2.753(1), 2.826(1), and 2.811(1) Å. The bridging SO_2 ligands are not coplanar with the Pt_3 triangle. The cluster shows indications of being sterically crowded with the $Pt\{Ph_2P(CH_2)_3PPh_2\}$ moiety adopting a low-symmetry conformation with respect to the Pt_3 plane. Proton-decoupled ^{31}P and ^{195}Pt n.m.r. studies have demonstrated that this low-symmetry conformation which makes the $P(C_6H_{11})_3$ ligands inequivalent is maintained in solution at low temperatures.

Since the pioneering work of Chatt and Chini[1] a large number of triangular clusters of platinum and related metals have been characterised.[2] Interestingly these clusters can either have a total of 42 or 44 electrons and some typical examples are summarised below (C_6H_{11} = cyclohexyl). It is apparent that

42 Electron
$[Pt_3(\mu\text{-}CO)_3\{P(C_6H_{11})_3\}_3]$ (ref. 3)
$[Pt_3(\mu\text{-}SO_2)_3(PPh_3)_3]$ (ref. 4)
$[Pt_3(\mu\text{-}H)_3H_3(PBu^t_3)_3]$ (ref. 5)
$[Rh_3(\mu\text{-}H)_3\{P(OMe)_3\}_6]$ (ref. 6)

44 Electron
$[Pt_3(\mu\text{-}CO)_3\{P(C_6H_{11})_3\}_4]$ (ref. 7)
$[Pt_3(\mu\text{-}CO)_3(PPh_3)_4]$ (ref. 1)
$[Pt_3(\mu\text{-}CO)_6]^{2-}$ (ref. 8)
$[Pd_3(\mu\text{-}SO_2)_2(CNBu^t)_5]$ (ref. 9)

both steric and electronic factors are responsible for discriminating between the alternative electron counts. Only in some instances has it proved possible to isolate both the 42- and 44-electron species, *e.g.* $[Pt_3(\mu\text{-}CO)_3\{P(C_6H_{11})_3\}_3]$. For this and the related compound $[Pt_3(\mu\text{-}CO)_3\{P(C_6H_{11})_3\}_4]$ some preliminary crystallographic data have been reported.[7] Molecular orbital calculations have suggested that the π-acceptor qualities of the bridging and terminal ligands play an important role in influencing the relative stabilities of the 42- and 44-electron species.[10]

An alternative mode of stabilising the 44-electron species relative to the 42 could be provided by utilising the chelating effect of bidentate tertiary phosphines. Therefore, it was decided to investigate the reactions of $[Pt_3(\mu\text{-}CO)_3\{P(C_6H_{11})_3\}_3]$ and $[Pt_3(\mu\text{-}SO_2)_3\{P(C_6H_{11})_3\}_3]$ with 1,2-bis(diphenylphosphino)ethane (dppe) and 1,3-bis(diphenylphosphino)propane (dppp).

Results and Discussion

The reactions of dppp with $[Pt_3(\mu\text{-}CO)_3\{P(C_6H_{11})_3\}_3]$ and $[Pt_3(\mu\text{-}SO_2)_3\{P(C_6H_{11})_3\}_3]$ are summarised in Scheme 1. A similar sequence of reactions was observed for dppe; however, the resultant products proved to be less stable and therefore were not investigated in such detail. The reactions of dppp with $[Pt_3(\mu\text{-}CO)_3\{P(C_6H_{11})_3\}_3]$ and $[Pt_3(\mu\text{-}SO_2)_3\{P(C_6H_{11})_3\}_3]$ occur immediately the solutions are mixed and the resultant products are obtained in high yield (> 70%) as crystalline solids. It is important not to exceed the stoicheiometric ratio of phosphine to cluster since under these conditions cluster degradation products are obtained. The compound $[Pt_3(\mu\text{-}SO_2)_3\{P(C_6H_{11})_3\}_2(dppp)]$ is dichroic, appearing green to reflected light and red to transmitted light.

The $^{31}P\text{-}\{^1H\}$ n.m.r. spectrum of $[Pt_3(\mu\text{-}CO)_3\{P(C_6H_{11})_3\}_2(dppp)]$ shows two resonances at 67.3 and 15.9 p.p.m. with respect to trimethyl phosphate arising from the $P(C_6H_{11})_3$ and dppp phosphorus atoms respectively. The $^{195}Pt\text{-}\{^1H\}$ n.m.r. spectrum shows two resonances at −4 060 [d, ^1J(Pt–P) = 4 854] and −3 708 p.p.m. [t, ^1J(Pt–P) = 3 422 Hz] with respect to $Na_2[PtCl_6]$. The former arises from the platinum atoms with $P(C_6H_{11})_3$ ligands co-ordinated and the latter from that with

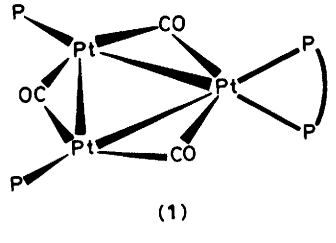

(1)

---

† *Supplementary data available* (No. SUP 56159, 28 pp.): full bond distances and angles, thermal parameters. See Instructions for Authors, *J. Chem. Soc., Dalton Trans.*, 1985, Issue 1, pp. xvii—xix. Structure factors are available from the editorial office.

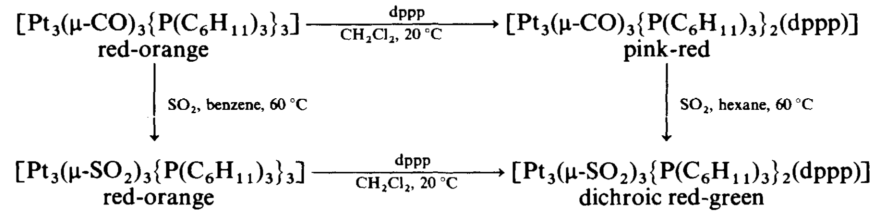

Scheme 1.

Table 1. Observed chemical shifts (δ/p.p.m.) and coupling constants (J/Hz) for $[Pt_3(\mu\text{-}CO)_3\{P(C_6H_{11})_3\}_2(dppp)]$

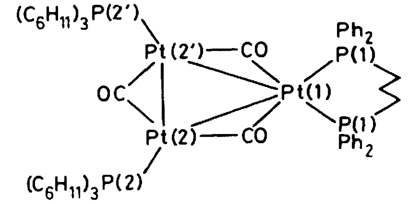

(*a*) Chemical shifts

P(1)	P(2)	Pt(1)	Pt(2)
15.9	67.3	−3 708	−4 060

(*b*) Coupling constants

	Pt(2′)	Pt(2)	Pt(1)	P(2′)	P(2)
P(1)	270	270	3 422	19	19
P(2)	510	4 854	429	60	
P(2′)	4 854	510	429		
Pt(1)	684	684			
Pt(2)	*				

* Value not measurable due to the broadness of ^{195}Pt resonance.

the diphosphine co-ordinated. This is consistent with a structure where the $P(C_6H_{11})_3$ phosphorus atoms lie in the plane of the triangle and the diphosphine ligand bonds in a symmetrical chelating manner in a plane perpendicular to the platinum triangle, (**1**). This structure is analogous to those studied by Venanzi and co-workers[11] having the formula $[Pt_3(\mu\text{-}CO)_3L_4]$ [L = PEt_3, PMe_2Ph, $PMePh_2$, PEt_2Bu^t, or $P(CH_2Ph)Ph_2$]. The coupling constants (see Table 1) are also comparable to those found in this series of compounds.

The $^{31}P\text{-}\{^1H\}$ and $^{195}Pt\text{-}\{^1H\}$ spectra of $[Pt_3(\mu\text{-}SO_2)_3\{P(C_6H_{11})_3\}_2(dppp)]$ are more complex than those discussed above for $[Pt_3(\mu\text{-}CO)_3\{P(C_6H_{11})_3\}_2(dppp)]$ and in addition are temperature dependent. The $^{31}P\text{-}\{^1H\}$ n.m.r. spectrum of $[Pt_3(\mu\text{-}SO_2)_3\{P(C_6H_{11})_3\}_2(dppp)]$ at 80 °C shows three resonances of relative intensity 2:1:1 centred at 36.6, 33.5, and −16.9 p.p.m. The $^{195}Pt\text{-}\{^1H\}$ spectrum at this temperature has a doublet at −5 197 p.p.m. and a doublet of doublets at −3 520 p.p.m. These data are consistent with co-ordination of dppp to a platinum atom of the cluster, but in such a fashion that the phosphorus atoms are not equivalent. The observed and calculated $^{31}P\text{-}\{^1H\}$ spectra are shown in Figure 1. The coupling constants for the high-temperature limit are given in Table 2. As the temperature is lowered the resonance at −5 197 p.p.m. broadens and splits into two doublets at −5 005 and −5 430 p.p.m. at −60 °C. The corresponding $^{31}P\text{-}\{^1H\}$ spectrum also shows increased complexity as the temperature is reduced. These data suggest that as the temperature is lowered an intramolecular fluxional process which averages the $P(C_6H_{11})_3$ environments is being frozen out. In order to understand the nature of this process more fully a single-crystal *X*-ray crystallographic analysis of $[Pt_3(\mu\text{-}SO_2)_3\{P(C_6H_{11})_3\}_2(dppp)]$ was undertaken. The relevant details of the structural analysis are given in the Experimental section. Selected intramolecular bond lengths and angles are given in Table 3. The fractional co-ordinates of the non-hydrogen atoms are given in Table 4. The structure of the molecule is illustrated in Figures 2 and 3.

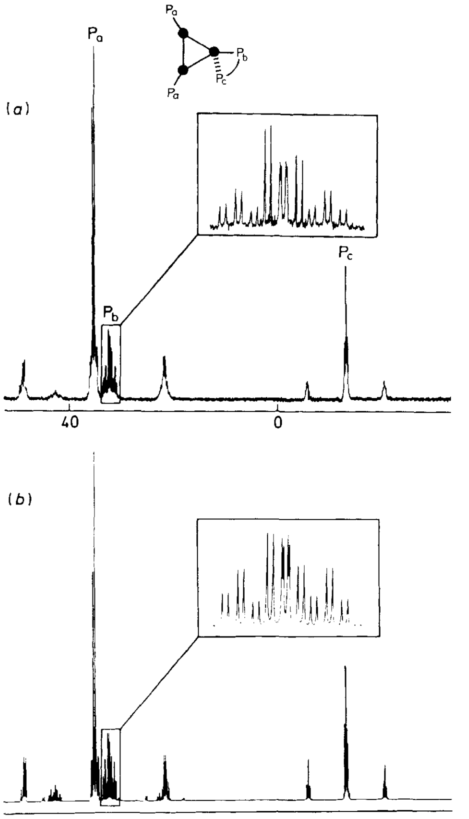

Figure 1. (*a*) Observed and (*b*) calculated $^{31}P\text{-}\{^1H\}$ spectra for $[Pt_3(\mu\text{-}SO_2)_3\{P(C_6H_{11})_3\}_2(dppp)]$

The platinum atoms form an approximately isosceles triangle with Pt–Pt distances of 2.753(1), 2.811(1), and 2.826(1) Å. These are significantly longer than the Pt–Pt distances in comparable trinuclear platinum cluster compounds.[3–5,7] This may be attributed in part to the large radius of the bridging sulphur atoms. The two tricyclohexylphosphine phosphorus atoms lie approximately in the plane of the metal triangle along with one of the phosphorus atoms of the chelating dppp. The second diphosphine phosphorus atom, P(3), lies well below the plane of the triangle. The Pt(3)–P(3) distance of 2.376(7) Å is significantly longer than the other Pt–P distances [2.265(6)—2.297(6) Å]. The P–Pt–P plane makes an angle of 66.1° with the metal plane; consequently the four phosphorus atoms are in chemically distinct environments in agreement with the low-temperature n.m.r. data. Two of the SO_2 units lie above the plane of the

Table 2. Observed chemical shifts (δ/p.p.m.) and coupling constants (*J*/Hz) for $[Pt_3(\mu\text{-}SO_2)_3\{P(C_6H_{11})_3\}_2(dppp)]$

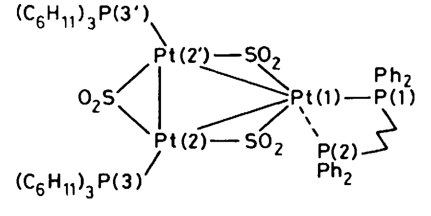

(*a*) Chemical shifts [a]

P(1)	P(2)	P(3)	Pt(1)	Pt(2)
33.5	−16.9	36.6	−3 520	−5 197

(*b*) Coupling constants

	Pt(2′)	Pt(2)	Pt(1)	P(3′)	P(3)	P(2)
P(1)	320	320	3 715	56	56	22
P(2)	95	95	2 659	0	0	
P(3)	179	4 802	28	18		
P(3′)	4 802	179	28			
Pt(1)	452	452				
Pt(2)	*b*					

[a] Measured from the high-temperature limit. [b] Value not measurable due to the broadness of ^{195}Pt resonance.

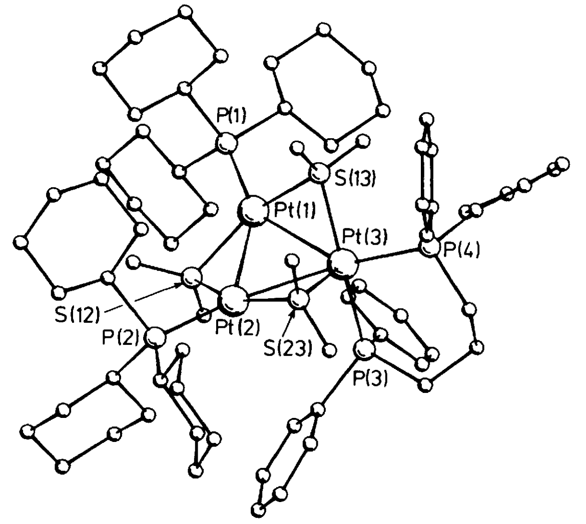

Figure 2. The molecular geometry of $[Pt_3(\mu\text{-}SO_2)_3\{P(C_6H_{11})_3\}_2(dppp)]$

metal triangle and one lies below. The Pt–S distances are comparable to these found in other Pt–SO_2 cluster compounds,[4,12,13] and the bond lengths show a small but significant asymmetry associated with the co-ordination of the SO_2 ligands.

Although the solid-state structure is consistent with the low-temperature $^{195}Pt\text{-}\{^1H\}$ n.m.r. spectra, the spectra are temperature dependent. The $Pt\{P(C_6H_{11})_3\}$ resonances coalesce at *ca.* 20 °C and are observed as a sharp doublet at 80 °C. The resonances associated with the phosphorus atoms of the diphosphine ligand are not averaged in this temperature range. These data suggest that the cluster is undergoing the intramolecular flipping process shown in Scheme 2. An activation energy, $\Delta G^{\neq}$ = *ca.* 45 kJ mol^{-1}, has been estimated for this process from the $^{195}Pt\text{-}\{^1H\}$ variable-temperature n.m.r. data.

Table 3. Selected molecular dimensions for $[Pt_3(\mu\text{-}SO_2)_3\{P(C_6H_{11})_3\}_2(dppp)]$ with estimated standard deviations in parentheses

(*a*) Intramolecular distances (Å)

Pt(1)–Pt(2)	2.753(1)	Pt(1)–P(1)	2.265(6)
Pt(1)–Pt(3)	2.826(1)	Pt(2)–P(2)	2.280(7)
Pt(2)–Pt(3)	2.811(1)	Pt(3)–P(3)	2.376(7)
		Pt(3)–P(4)	2.297(6)
S(12)–O(121)	1.48(2)		
S(12)–O(122)	1.43(2)	Pt(1)–S(13)	2.246(6)
S(13)–O(131)	1.47(2)	Pt(3)–S(13)	2.294(6)
S(13)–O(132)	1.44(2)	Pt(1)–S(12)	2.242(7)
S(23)–O(231)	1.48(2)	Pt(2)–S(12)	2.312(6)
S(23)–O(232)	1.42(2)	Pt(2)–S(23)	2.281(6)
		Pt(3)–S(23)	2.390(7)

(*b*) Bond angles (°)

Pt(1)–Pt(3)–Pt(2)	58.47(4)	S(13)–Pt(3)–S(23)	103.6(2)
Pt(1)–Pt(2)–Pt(3)	61.04(4)	P(3)–Pt(3)–S(13)	154.0(2)
Pt(2)–Pt(1)–Pt(3)	60.48(4)	P(3)–Pt(3)–S(23)	98.5(2)
		P(4)–Pt(3)–S(13)	92.6(2)
S(12)–Pt(1)–S(13)	150.9(2)	P(4)–Pt(3)–S(23)	101.6(2)
P(1)–Pt(1)–S(12)	102.8(2)	P(3)–Pt(3)–P(4)	96.4(2)
P(1)–Pt(1)–S(13)	105.1(2)		
		Pt(1)–S(13)–Pt(3)	77.0(2)
S(12)–Pt(2)–S(23)	157.3(2)	Pt(1)–S(12)–Pt(2)	74.4(2)
P(2)–Pt(2)–S(12)	94.4(2)	Pt(2)–S(23)–Pt(3)	73.9(2)
P(2)–Pt(2)–S(23)	107.3(2)		

Angles (°) between the plane Pt(1)–Pt(2)–Pt(3) and other planes

Pt(1)–S(13)–Pt(3)	52.1	Pt(2)–S(23)–Pt(3)	38.2
Pt(1)–S(12)–Pt(2)	38.7	P(3)–Pt(3)–P(4)	66.1

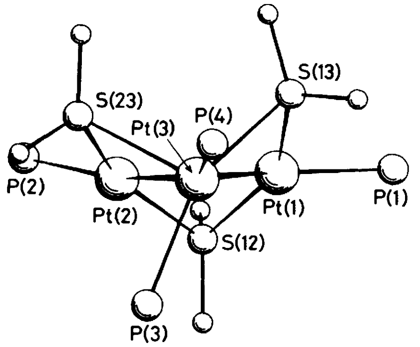

Figure 3. Illustration of the inner co-ordination sphere of $[Pt_3(\mu\text{-}SO_2)_3\{P(C_6H_{11})_3\}_2(dppp)]$

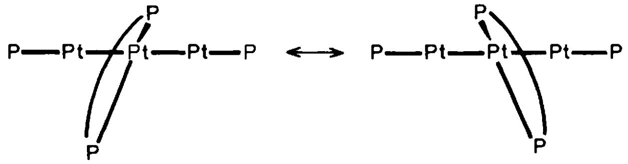

Scheme 2.

X-Ray structural determinations on $[Pt_3(\mu\text{-}CO)_3\{P(C_6H_{11})_3\}_3]$[3] and $[Pt_3(\mu\text{-}SO_2)_3(PPh_3)_3]$ have shown them to be essentially planar. If the bridged metal–metal bonds are ignored then these clusters can be viewed in terms of three T-shaped ML_3 fragments sharing common bridging groups, structure (2). The S–Pt–S bond angles in $[Pt_3(\mu\text{-}SO_2)_3(PPh_3)_3]$ have an average of 166° which is similar to the P–Rh–P bond angle reported for the T-shaped d^8 complex $[Rh(PPh_3)_3]^+$

Table 4. Final fractional co-ordinates for non-hydrogen atoms with estimated standard deviations in parentheses

Atom	*X/a*	*Y/b*	*Z/c*	Atom	*X/a*	*Y/b*	*Z/c*
Pt(1)	0.746 5(1)	0.114 14(2)	0.794 29(6)	C(231)	0.715(2)	0.070 8(5)	0.477(1)
Pt(2)	0.754 6(1)	0.128 81(2)	0.630 78(6)	C(232)	0.584(2)	0.082 2(5)	0.465(1)
Pt(3)	0.708 5(1)	0.178 02(2)	0.739 31(6)	C(233)	0.498(2)	0.053 1(7)	0.450(2)
P(1)	0.754 7(6)	0.079 3(2)	0.901 3(4)	C(234)	0.522(3)	0.034 8(8)	0.373(2)
P(2)	0.820 2(6)	0.101 8(2)	0.524 6(4)	C(235)	0.656(3)	0.024 6(6)	0.380(2)
P(3)	0.515 5(6)	0.184 6(2)	0.659 6(4)	C(236)	0.742(2)	0.054 0(7)	0.398(2)
P(4)	0.727 4(6)	0.229 6(1)	0.788 6(4)	C(311)	0.461(2)	0.164 6(5)	0.560(1)
S(12)	0.674 5(6)	0.083 8(1)	0.684 7(4)	C(312)	0.373(2)	0.140 6(6)	0.555(1)
S(13)	0.839 6(6)	0.158 5(1)	0.849 0(4)	C(313)	0.324(2)	0.127 8(6)	0.477(1)
S(23)	0.826 5(6)	0.179 9(1)	0.629 0(4)	C(314)	0.359(2)	0.140 1(6)	0.405(1)
O(121)	0.740(2)	0.053 7(4)	0.674(1)	C(315)	0.449(2)	0.163 4(6)	0.410(1)
O(122)	0.546(2)	0.081 5(5)	0.664(1)	C(316)	0.501(2)	0.175 9(6)	0.488(1)
O(131)	0.969(2)	0.158 5(4)	0.845(1)	C(321)	0.406(2)	0.172 8(5)	0.725(1)
O(132)	0.811(1)	0.171 5(4)	0.926(1)	C(322)	0.294(2)	0.189 0(6)	0.721(2)
O(231)	0.762(2)	0.202 9(4)	0.570(1)	C(323)	0.208(2)	0.178 4(7)	0.769(2)
O(232)	0.952(2)	0.184 8(4)	0.654(1)	C(324)	0.231(2)	0.152 0(6)	0.819(2)
C(111)	0.909(2)	0.062 4(5)	0.936(1)	C(325)	0.343(2)	0.135 8(6)	0.823(1)
C(112)	0.957(2)	0.047 2(6)	0.861(1)	C(326)	0.428(2)	0.145 8(6)	0.774(2)
C(113)	1.082(2)	0.032 0(6)	0.891(2)	C(341)	0.478(2)	0.226 1(6)	0.627(2)
C(114)	1.168(2)	0.058 3(7)	0.929(2)	C(342)	0.510(2)	0.252 2(6)	0.696(2)
C(115)	1.118(2)	0.074 0(7)	1.003(2)	C(343)	0.650(2)	0.259 2(6)	0.715(1)
C(116)	0.994(2)	0.088 8(5)	0.975(2)	C(411)	0.669(2)	0.238 2(5)	0.883(1)
C(121)	0.714(2)	0.098 5(5)	0.992(1)	C(412)	0.701(2)	0.266 2(5)	0.930(1)
C(122)	0.602(2)	0.119 9(6)	0.976(1)	C(413)	0.641(2)	0.273 8(6)	0.997(2)
C(123)	0.590(3)	0.139 9(6)	1.055(2)	C(414)	0.546(2)	0.255 4(7)	1.015(2)
C(124)	0.576(3)	0.116 9(8)	1.129(2)	C(415)	0.514(2)	0.227 8(7)	0.970(2)
C(125)	0.689(3)	0.095 8(6)	1.148(1)	C(416)	0.580(2)	0.218 4(6)	0.906(2)
C(126)	0.708(2)	0.076 3(5)	1.069(1)	C(421)	0.881(2)	0.244 0(6)	0.808(1)
C(131)	0.663(2)	0.043 6(5)	0.868(1)	C(422)	0.933(2)	0.257 2(7)	0.742(1)
C(132)	0.684(2)	0.013 3(6)	0.922(1)	C(423)	1.056(2)	0.265 5(8)	0.754(2)
C(133)	0.605(2)	−0.014 3(5)	0.878(2)	C(424)	1.126(2)	0.260 0(8)	0.832(2)
C(134)	0.471(2)	−0.005 2(6)	0.861(2)	C(425)	1.076(2)	0.247 1(8)	0.898(2)
C(135)	0.451(2)	0.025 7(6)	0.809(1)	C(426)	0.952(2)	0.238 6(7)	0.885(1)
C(136)	0.528(2)	0.052 5(5)	0.855(1)	C(1)	1.158(4)	0.067(1)	1.256(3)
C(211)	0.865(2)	0.124 6(5)	0.438(1)	C(2)	1.036(4)	0.071 9(8)	1.238(3)
C(212)	0.974(2)	0.146 8(6)	0.462(1)	C(3)	0.957(3)	0.047 9(9)	1.252(2)
C(213)	1.013(2)	0.160 6(6)	0.382(2)	C(4)	1.003(3)	0.020 3(8)	1.293(3)
C(214)	0.911(2)	0.181 1(6)	0.338(2)	C(5)	1.126(3)	0.016 2(8)	1.314(2)
C(215)	0.797(2)	0.160 6(7)	0.315(1)	C(6)	1.202(3)	0.041(1)	1.301(3)
C(216)	0.756(2)	0.144 6(6)	0.392(2)	C(7)	0.048(3)	0.168(1)	0.069(2)
C(221)	0.959(2)	0.077 6(6)	0.570(1)	C(8)	0.068(3)	0.157 5(9)	0.149(2)
C(222)	1.037(2)	0.096 4(5)	0.639(1)	C(9)	0.184(3)	0.155 9(9)	0.191(2)
C(223)	1.136(2)	0.073 6(6)	0.683(1)	C(10)	0.281(3)	0.163(1)	0.152(2)
C(224)	1.212(2)	0.061 2(7)	0.619(2)	C(11)	0.261(3)	0.173(1)	0.069(2)
C(225)	1.133(3)	0.041 9(6)	0.552(2)	C(12)	0.144(3)	0.174 8(9)	0.028(2)
C(226)	1.036(2)	0.064 2(7)	0.505(1)				

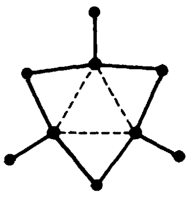

(2)

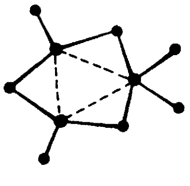

(3)

(159.3°).[14] A preliminary report of the structure of [$Pt_3(\mu$-$CO)_3\{P(C_6H_{11})_3\}_4$][7] suggests that this cluster has a related geometry with one of the T-shaped fragments replaced by a C_{2v} trigonal-bipyramidal fragment as shown in (**3**).

This contrasts with the distinctly non-planar geometries observed for [$Rh_3(\mu$-$H)_3\{P(OMe)_3\}_6$],[6] [$Pd_3(\mu$-$SO_2)_2(CNBu^t)_5$],[9] and in the present structure. In the former examples the addition of more terminal ligands results in the conversion of T-shaped fragments into square-planar fragments and a decrease in the (μ-X)–metal–(μ-X) (X = H, CO, or SO_2) bond angle from *ca.* 180 to *ca.* 90°. The smaller angles subtended at the metal atoms necessitate a folding of the $M_3(\mu$-$X)_3$ ring and account for the geometries illustrated in (**4**) and (**5**).

The structure of [$Pt_3(\mu$-$SO_2)_3\{P(C_6H_{11})_3\}_2$(dppp)] does not conform to either of these patterns. The local geometry about the PtS_2(dppp) moiety most closely resembles a square pyramid with a missing vertex, structure (**6**). The adoption of this square-pyramidal geometry is associated with a dramatic difference in the S–Pt–S bond angles, *viz.* 150.9(2) and 157.3(2)° for the angles about Pt(1) and Pt(2) and 103.6(2)° for the angle about Pt(3). This bond angle change is the primary cause of the observed non-planar geometry. The remaining bond angles about Pt(3), *i.e.* P(4)–Pt(3)–P(3) 96.4(2), P(4)–Pt(3)–S(13) 92.6(2), P(4)–Pt(3)–S(23) 101.6(2), P(3)–Pt(3)–S(23) 98.5(2), and P(3)–Pt(3)–S(13) 154.0(2)°, are consistent with the proposed distorted square-pyramidal co-ordination.

It is difficult to ascribe the observed structural difference between [$Pt_3(\mu$-$CO)_3\{P(C_6H_{11})_3\}_4$] and [$Pt_3(\mu$-$SO_2)_3$-$\{P(C_6H_{11})_3\}_2$(dppp)] to anything but steric effects since both of these molecules are clearly very crowded (see, for example,

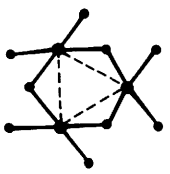

(4)

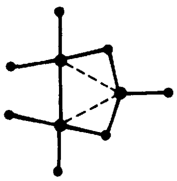

(5)

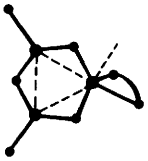

(6)

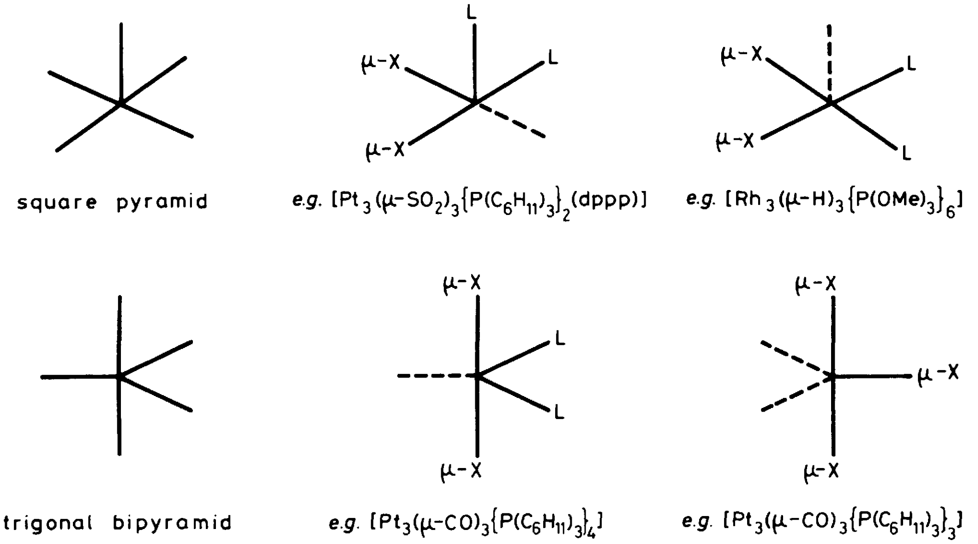

Figure 4. Local co-ordination geometries of fragments in triangular clusters of the platinum metals and their relationships to the square pyramid and trigonal bipyramid

Figure 2). Nevertheless, comparison of the related cluster compounds described above strongly suggests that bridged metal–metal bonds do not exert a strong stereochemical influence. The local co-ordination geometries are all based on fragments derived from idealised trigonal-bipyramidal or square-pyramidal units as shown in Figure 4. Interestingly these fragment geometries are those which in mononuclear compounds would be favoured for d^8 configurations, suggesting that localised two-centre two-electron bonds are being formed between the metal atom and the bridging ligands. Similar considerations are relevant to the discussion of the structures of carbonyl clusters of the earlier platinum metals where, for example, when the metals have an effective d^6 electron configuration octahedral and square-pyramidal local co-ordination geometries are observed.[15]

Experimental

Reactions were routinely carried out, using standard Schlenk-line procedures, under an atmosphere of pure, dry N_2 and using dry dioxygen-free solvents. Microanalyses (C and H) were carried out by Mr. M. Gascoyne and his staff of this laboratory. Infrared spectra were recorded as Nujol mulls using a Pye-Unicam SP2000 spectrometer.

Proton-decoupled ^{31}P and ^{195}Pt n.m.r. spectra were recorded using a Bruker AM-250 spectrometer. Samples for $^{31}P\text{-}\{^1H\}$ were referenced to $P(OMe)_3O$ in D_2O and $^{195}Pt\text{-}\{^1H\}$ to $Na_2[PtCl_6]$ in D_2O. The machine operating frequencies were 101.26 MHz for ^{31}P and 53.55 MHz for ^{195}Pt. All samples were run in deuteriated solvents. N.m.r. computer simulations were carried out using the Oxford University VAX computer system using a program developed by Professor R. K. Harris of the University of East Anglia and adapted for use at Oxford by Dr. A. E. Derome. $[Pt_3(\mu\text{-}CO)_3\{P(C_6H_{11})_3\}_3]$ was synthesised by the method of Clark *et al.*[16] from *trans*-$[PtH_2\{P(C_6H_{11})_3\}_2]$ and CO.

Synthesis of $[Pt_3(\mu\text{-}CO)_3\{P(C_6H_{11})_3\}_2(dppp)]$.—$[Pt_3(\mu\text{-}CO)_3\{P(C_6H_{11})_3\}_3]\cdot C_6H_6$ (0.3 g, 0.2 mmol) was dissolved in benzene (20 cm^3) and dppp (0.078 g, 0.2 mmol) was added with stirring. The resulting pink-red solution was stirred for a further 10 min. On addition of ethanol (40 cm^3) to this solution and removal of the benzene *in vacuo* a pink solid was obtained. This was recrystallised from dichloromethane–methanol to yield the *product* (0.27 g, 87%) as pink crystals (Found: C, 48.5; H, 5.8. $C_{66}H_{92}O_3P_4Pt_3$ requires C, 48.3; H, 5.6%); ν(CO) at 1 842m, 1 790s, 1 763s, and 1 734w cm^{-1}.

Synthesis of $[Pt_3(\mu\text{-}SO_2)_3\{P(C_6H_{11})_3\}_2(dppp)]$.—$[Pt_3(\mu\text{-}CO)_3\{P(C_6H_{11})_3\}_3]\cdot C_6H_6$ (0.3 g, 0.2 mmol) was dissolved in hexane (40 cm^3) and dppp (0.078 g, 0.2 mmol) was added with stirring. Sulphur dioxide was bubbled through the resultant pink-red solution which was immediately decolourised and a cream-coloured precipitate was deposited. The stream of SO_2 was passed through the solution for 30 min and on heating the solution to 60 °C the solid gradually became green during this time. This solid was filtered off and washed in turn with cold hexane (40 cm^3) and cold ethanol (20 cm^3). Recrystallisation from dichloromethane–benzene–light petroleum (b.p. 100—120 °C) yielded black-green crystals (red by transmitted light) of the *product* (dibenzene solvate) (0.27 g, 75%) (Found: C, 48.1; H, 5.8. $C_{63}H_{92}O_6P_4Pt_3S_3\cdot 2C_6H_6$ requires C, 47.2; H, 5.5%); $\nu(SO_2)$ at 1 237s, 1 210s, 1 186s, 1 098m, 1 080s, 1 050s, and 1 042s cm^{-1}.

Crystal Data.—$C_{63}H_{92}O_6P_4Pt_3S_3\cdot 2C_6H_6$, M = 1 906.7, monoclinic, a = 11.244(6), b = 41.746(3), c = 16.324(2) Å, β = 98.51(3)°, U = 7 578 Å^3 (by least-squares refinement on diffractometer angles for 25 automatically centred reflections, λ = 1.5418 Å), space group $P2_1/n$, D_m = 1.63, Z = 4, D_c = 1.67 g cm^{-3}. Green-black crystals were grown from CH_2Cl_2–benzene–light petroleum (b.p. 100—120 °C) and mounted on a glass fibre. Crystal dimensions 0.1 × 0.07 × 0.05 mm, μ(Cu-K_α) = 122.7 cm^{-1}.

Geometric diffraction data were collected on a CAD4 diffractometer: $\omega/2\theta$ with ω scan width 0.8°, graphite-monochromated Cu-K_α radiation; 9 340 reflections measured ($1.5 < \theta < 60°$), 4 506 unique absorption-corrected reflections with $I \geqslant 3\sigma(I)$, merging R = 0.0343.

The structure was solved by direct methods (MULTAN) (Pt atoms) followed by normal heavy-atom procedures. Refinement was by blocked-matrix least-squares methods, with Pt, P, and S atoms anisotropic and the remainder isotropic. A Chebyshev weighting scheme with coefficients of 46.8, 67.7, 30.6, and 5.1 gave satisfactory agreement analyses. Final R and R' values are 0.0600 and 0.0707. Programs and computers used and sources of scattering factor data are given in refs. 17—19.

References

1 J. Chatt and P. Chini, *J. Chem. Soc. A*, 1970, 1538.

2 F. R. Hartley, 'Comprehensive Organometallic Chemistry,' eds. G. Wilkinson, F. G. A. Stone, and E. W. Abel, Pergamon Press, Oxford, 1982, vol. 6, p. 471.

3 A. Albinati, *Inorg. Chim. Acta*, 1977, **22**, L31.

4 D. C. Moody and R. R. Ryan, *Inorg. Chem.*, 1977, **16**, 1052.

5 P. W. Frost, J. A. K. Howard, J. L. Spencer, D. G. Turner, and D. Gregson, *J. Chem. Soc., Chem. Commun.*, 1981, 1104.

6 R. K. Brown, J. M. Williams, A. J. Sivak, and E. L. Muetterties, *Inorg. Chem.*, 1980, **19**, 370.

7 A. Albinati, G. Carturan, and A. Musco, *Inorg. Chim. Acta*, 1976, **16**, L3.

8 G. Longoni and P. Chini, *J. Am. Chem. Soc.*, 1976, **98**, 7225.

9 S. Otsuka, Y. Tatsuno, M. Niki, T. Aoki, M. Matsumoto, H. Yoshioka, and K. Nakatsu, *J. Chem. Soc., Chem. Commun.*, 1973, 445.

10 J. W. Lauher, *J. Am. Chem. Soc.*, 1978, **100**, 5305; J. Evans, *J. Chem. Soc., Dalton Trans.*, 1980, 1005.

11 A. Moor, P. S. Pregosin, and L. M. Venanzi, *Inorg. Chim. Acta*, 1981, **61**, 135.

12 D. G. Evans, G. R. Hughes, D. M. P. Mingos, J-M. Bassett, and A. J. Welch, *J. Chem. Soc., Chem. Commun.*, 1980, 1255.

13 C. E. Briant, D. G. Evans, and D. M. P. Mingos, *J. Chem. Soc., Chem. Commun.*, 1982, 1144.

14 Y. W. Yared, S. L. Miles, R. Bau, and C. A. Reed, *J. Am. Chem. Soc.*, 1977, **99**, 7076.

15 J. A. Jensen, D. E. Fjare, and W. L. Gladfelter, *Inorg. Chem.*, 1983, **22**, 1250.

16 H. C. Clark, A. B. Goel, and C. S. Wong, *Inorg. Chim. Acta*, 1977, **34**, 159.

17 Crystals User Manual, J. R. Carruthers, Oxford University Computing Centre, 1975.

18 CHEMGRAF User Manual, K. Davies, Chemical Crystallography Laboratory, Oxford, 1981.

19 'International Tables for *X*-Ray Crystallography,' Kynoch Press, Birmingham, 1974, vol. 4, p. 99.

Received 20*th July* 1984; *Paper* 4/1255